Quantum Information and Computation, Vol. 15, No. 13&14 (2015) 1248–1258

LIMIT DISTRIBUTIONS FOR DIFFERENT FORMS OF FOUR-STATE QUANTUM WALKS ON A TWO-DIMENSIONAL LATTICE

TAKUYA MACHIDA
Research Fellow of Japan Society for the Promotion of Science,
Meiji University, Nakano Campus, 4-21-1 Nakano, Nakano-ku, Tokyo 164-8525, Japan

C.M. CHANDRASHEKAR
Optics and Quantum Information Group, The Institute of Mathematical Sciences
CIT Campus, Taramani, Chennai, India - 600113

NORIO KONNO
Department of Applied Mathematics, Faculty of Engineering, Yokohama National University,
Hodogaya, Yokohama, 240-8501, Japan

THOMAS BUSCH
Quantum Systems Unit, Okinawa Institute of Science and Technology Graduate University,
Okinawa, Japan

Received March 25, 2015
Revised July 2, 2015

Long-time limit distributions are key quantities for understanding the asymptotic dynamics of quantum walks, and they are known for most forms of one-dimensional quantum walks using two-state coin systems. For two-dimensional quantum walks using a four-state coin system, however, the only known limit distribution is for a walk using a parameterized Grover coin operation and analytical complexities have been a major obstacle for obtaining long-time limit distributions for other coins. In this work however, we present two new types of long-time limit distributions for walks using different forms of coin-flip operations in a four-state coin system. This opens the road towards understanding the dynamics and asymptotic behaviour for higher state coin system from a mathematical view point.

Keywords: discrete-time quantum walk, 2-dimensional lattice, limit distribution
Communicated by: R Cleve & R Laflamme

1 Introduction

The quantum mechanical analogue to the discrete-time random walk is the discrete-time quantum walk [1, 2, 3, 4, 5, 6, 7, 8], which evolves a single quantum state using discrete steps on a discrete lattice in a position space. The total quantum state for the walk is described on a tensor Hilbert space $\mathcal{H}_p \otimes \mathcal{H}_c$, where $\mathcal{H}_p$ and $\mathcal{H}_c$ are the position Hilbert space and the coin Hilbert space spanned by the position basis and the internal states of the walker, respectively. One of its main features is the fact that it creates a coherent superposition of the initial state at distinct lattice sites, which leads to an evolution through multiple paths

resulting in the interference effect dominating the dynamics. These interference effects result in a quadratically faster spread of the probability distribution compared to classical random walks [6, 7].

The dynamics of quantum walks on a one-dimensional lattice using different forms of two state coin operations has been exactly analyzed and a lot of long-time limit theorems have been reported [9]. With increase in the size of both, the position Hilbert space and coin Hilbert space, the numerical simulations are limited by the computational power, and experimental demonstrations are limited by precise control over the physical system with a higher dimensional coin space. Using a two-particle system [10, 11, 12, 13], few configurations of higher dimensional quantum walks have been experimentally implemented. In these experimental realizations, higher dimensional walks are in the form of two-correlated particles on a one- and two-dimensional position space. No experimental realization on a single particle system with four coin states has been achieved yet. Therefore, long time limit theorems are the best possible approach for understanding the asymptotic behaviour of walks with higher dimensional coin space. However, due to difficulties in the mathematical analysis of two-dimensional walks with four internal states, the long-time limit behaviour has until now only been studied and analyzed for one form of a walk parameterized by a special coin-flip operator which includes the Grover coin [14]. In this work we focus mainly on the mathematical treatment of quantum walks on a two-dimensional square lattice and present the analytical form of the long-time behavior of the walk using different forms of coin-flip operators. The new theorems we present will reveal new properties of the quantum walk on a two-dimensional lattice, which holds the potential for exploiting these properties for quantum algorithms and other applications.

In the next section we will define the standard two-dimensional quantum walk with a four-state system and in Sec. 3 we first briefly review a walk using the Grover coin and present long-time limit theorems for two-dimensional quantum walks with two different forms of coin-flip operators recently introduced in Ref. [15]. These new forms of the operators are very different from the parameterized coin-flip operator used in [14]. The proofs of the two limit theorems are presented in the same section and we conclude with a summary in Sec. 4.

2 Quantum walk on a two-dimensional lattice

A standard quantum walk on a two-dimensional lattice is defined on a Hilbert space which is a tensor space of a position space and a coin space. For a walker with a four-state coin, the position space $\mathcal{H}_p$ is spanned by the basis $\{|x,y\rangle : x,y \in \mathbb{Z}\}$ and the coin space $\mathcal{H}_c$ is spanned by the basis $\{|l\rangle, |u\rangle, |d\rangle, |r\rangle\}$,

$$|l\rangle = \begin{bmatrix}1\\0\\0\\0\end{bmatrix}, \quad |u\rangle = \begin{bmatrix}0\\1\\0\\0\end{bmatrix}, \quad |d\rangle = \begin{bmatrix}0\\0\\1\\0\end{bmatrix}, \quad |r\rangle = \begin{bmatrix}0\\0\\0\\1\end{bmatrix}. \tag{1}$$

The entire state of the walker $|\Psi_t\rangle = \sum_{x,y\in\mathbb{Z}} |x,y\rangle \otimes |\psi_t(x,y)\rangle \in \mathcal{H}_p \otimes \mathcal{H}_c$ at time $t \in \{0,1,2,\ldots\}$ evolves to the next state $|\Psi_{t+1}\rangle$ by first applying an operator C, followed by a position-shift operator S,

$$|\Psi_{t+1}\rangle = SC\,|\Psi_t\rangle, \tag{2}$$

where

$$C = \sum_{x,y\in\mathbb{Z}} |x,y\rangle \langle x,y| \otimes U, \tag{3}$$

is an operator acting on both, the coin and the position space with a 4×4 unitary matrix U as the coin-flip operator acting on the coin space. The position-shift operator is given by

$$\begin{aligned} S = \sum_{x,y\in\mathbb{Z}} \Big(& |x-1,y\rangle \langle x,y| \otimes |l\rangle \langle l| + |x,y+1\rangle \langle x,y| \otimes |u\rangle \langle u| \\ & + |x,y-1\rangle \langle x,y| \otimes |d\rangle \langle d| + |x+1,y\rangle \langle x,y| \otimes |r\rangle \langle r| \Big). \end{aligned} \tag{4}$$

Equation (4) means that the position-shift operator S shifts the walker with the coin state $|l\rangle$ (resp. $|u\rangle, |d\rangle, |r\rangle$) to the left (resp. up, down, right). For a generic initial state given by

$$|\Psi_0\rangle = |0,0\rangle \otimes \Big(\alpha |l\rangle + \beta |u\rangle + \gamma |d\rangle + \delta |r\rangle \Big), \tag{5}$$

where α, β, γ and δ can be any complex numbers satisfying the condition $|\alpha|^2 + |\beta|^2 + |\gamma|^2 + |\delta|^2 = 1$, the probability distribution of the walker at time t is given by

$$\mathbb{P}\left[(X_t, Y_t) = (x,y)\right] = \langle \Psi_t | \left(|x,y\rangle \langle x,y| \otimes \sum_{j\in\{l,u,d,r\}} |j\rangle \langle j| \right) |\Psi_t\rangle, \tag{6}$$

where (X_t, Y_t) denotes the position of the walker after it has been observed at time t.

In the following we will present two forms of coin-flip operations different from the 4×4 Grover coin operation and analyze the probability distributions after a long time. Our result in the form of long-time limit theorem will show that the density function reveals features of the walk that are very different from the known features of the walk using the Grover coin.

3 Two types of limit distributions

For a general quantum walk of a four state system with the coin-flip operator given by

$$U = \begin{bmatrix} -p & q & \sqrt{pq} & \sqrt{pq} \\ q & -p & \sqrt{pq} & \sqrt{pq} \\ \sqrt{pq} & \sqrt{pq} & -q & p \\ \sqrt{pq} & \sqrt{pq} & p & -q \end{bmatrix}, \tag{7}$$

and $q = 1 - p$ ($p \in (0,1)$), its long-time limit distribution is well known [14]. For $p = q = \frac{1}{2}$, this parameterized operator takes the form of a Grover coin

$$U = \frac{1}{2} \begin{bmatrix} -1 & 1 & 1 & 1 \\ 1 & -1 & 1 & 1 \\ 1 & 1 & -1 & 1 \\ 1 & 1 & 1 & -1 \end{bmatrix}, \tag{8}$$

and hence the walk is commonly described as a Grover walk. The result of Watabe *et al.* [14] gives the information of the position of the walker on a space rescaled by time t and describes how the distribution converges as $t \to \infty$. The long time density function can be separated

into two parts, with one being a Dirac δ-function at the origin and the other a spread-out continuous function. The Dirac δ-function part implies that the walk strongly localises around the origin, whereas the continuous function has a quadratic compact support.

Let us briefly review a long-time limit distribution of the Grover walk, which was obtained by Watabe *et al.* [14] as

$$\begin{aligned}&\lim_{t\to\infty}\mathbb{P}\left(\frac{X_t}{t}\le x,\,\frac{Y_t}{t}\le y\right)\\&=\int_{-\infty}^{x}du\int_{-\infty}^{y}dv\left\{\Delta(\alpha,\beta,\gamma,\delta)\,\delta_o(u,v)+f(u,v)\eta(u,v;\alpha,\beta,\gamma,\delta)I_{\mathcal{D}}(u,v)\right\}.\end{aligned}\tag{9}$$

Here $\delta_o(x,y)$ is the Dirac δ-function at the origin and

$$\Delta(\alpha,\beta,\gamma,\delta)=1-M_1-\left(\frac{1}{2}-\frac{1}{\pi}\right)(M_4+M_5),\tag{10}$$

$$f(x,y)=\frac{2}{\pi^2(x+y+1)(x-y+1)(x+y-1)(x-y-1)},\tag{11}$$

$$\eta(x,y;\alpha,\beta,\gamma,\delta)=M_1-M_2x-M_3y+M_4x^2+M_5y^2+M_6xy,\tag{12}$$

with

$$M_1=\frac{1}{2}+\Re(\alpha\overline{\delta}+\beta\overline{\gamma}),\tag{13}$$

$$M_2=|\alpha|^2-|\delta|^2+\Re(-\alpha\overline{\beta}-\alpha\overline{\gamma}+\beta\overline{\delta}+\gamma\overline{\delta}),\tag{14}$$

$$M_3=-|\beta|^2+|\gamma|^2+\Re(\alpha\overline{\beta}-\alpha\overline{\gamma}+\beta\overline{\delta}-\gamma\overline{\delta}),\tag{15}$$

$$M_4=\frac{1}{2}(|\alpha|^2-|\beta|^2-|\gamma|^2+|\delta|^2)-\Re(\alpha\overline{\beta}+\alpha\overline{\gamma}+3\alpha\overline{\delta}+\beta\overline{\gamma}+\beta\overline{\delta}+\gamma\overline{\delta}),\tag{16}$$

$$M_5=-\frac{1}{2}(|\alpha|^2-|\beta|^2-|\gamma|^2+|\delta|^2)-\Re(\alpha\overline{\beta}+\alpha\overline{\gamma}+\alpha\overline{\delta}+3\beta\overline{\gamma}+\beta\overline{\delta}+\gamma\overline{\delta}),\tag{17}$$

$$M_6=-2\Re(-\alpha\overline{\beta}+\alpha\overline{\gamma}+\beta\overline{\delta}-\gamma\overline{\delta}),\tag{18}$$

$$I_{\mathcal{D}}(x,y)=\begin{cases}1 & \left(x^2+y^2<\frac{1}{2}\right),\\ 0 & (\text{otherwise}).\end{cases}\tag{19}$$

The notation $\Re(z)$ denotes the real part of the complex number z. The first part of the integral describes the localised part of the distribution and the non-localised part is given by $f(x,y)$, $\eta(x,y;\alpha,\beta,\gamma,\delta)$, and $I_{\mathcal{D}}(x,y)$. The probability distribution after $t=100$ evolution steps is shown in Fig. 1(a) and the delocalised part, obtained from the limit distribution, is displayed in Fig. 1(b).

In the following we will extend the study of two-dimensional quantum walks to two specific forms of coin-flip operations recently introduced to study nonrepeating forms of discrete-time quantum walks [15] and derive the long time limit density functions, which are fundamentally different from the one known for the Grover walk. Most strikingly they do not show localisation because both limit density functions consist of just a continuous function. One of these has a biquadratic compact support and the other has a quadratic compact support.

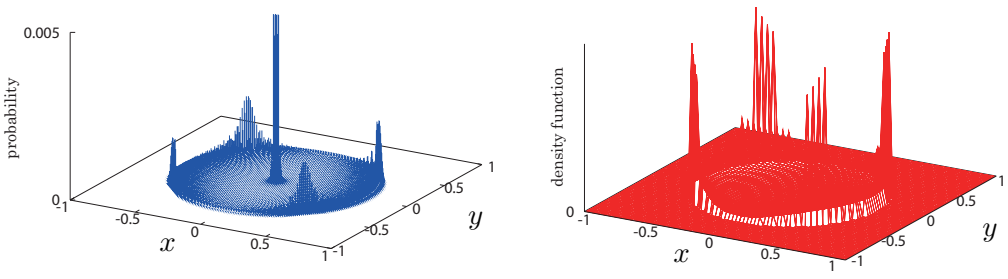

(a) $\mathbb{P}\left[\left(\frac{X_t}{t}, \frac{Y_t}{t}\right) = (x, y)\right]$ (b) $f(x,y)\eta(x,y)I_{\mathcal{D}}(x,y)$

Fig. 1. Grover walk: Figure (a) shows the probability distribution $\mathbb{P}\left[\left(\frac{X_t}{t}, \frac{Y_t}{t}\right) = (x, y)\right]$ at time $t = 100$. Figure (b) shows the function $f(x,y)\eta(x,y)I_{\mathcal{D}}(x,y)$ for $\alpha = -\delta = \frac{1}{2}$ and $\beta = \gamma = \frac{i}{2}$.

3.1 Biquadratic compact support type

First, we will consider a walk with a coin operation of the form

$$U = \frac{1}{\sqrt{3}} \begin{bmatrix} 0 & 1 & 1 & -1 \\ 1 & 0 & 1 & 1 \\ 1 & -1 & 0 & -1 \\ -1 & -1 & 1 & 0 \end{bmatrix}. \tag{20}$$

The probability distribution for this walk has recently been studied by Proctor *et al.* [15] and they referred to the coin operator given by Eq. (20) as a nonrepeating coin. Here, choosing the same coin operation, we describe an interesting result by analyzing the mathematical forms of the limiting functions. Their results suggest that this coin operator leads to a delocalisation of the quantum walk and it should therefore possess a limit distribution which is different from that of the quantum walk controlled by the parameterized Grover coin of Eq. (7). In fact, the limit theorem presented in the following, confirms the absence of a localised component of the walk not only for a particular initial state, but in general for any initial state at the origin.

Theorem 1 *For the quantum walk governed by the coin-flip operator given in Eq.* (20)*, the long-time limit distribution can be written as*

$$\begin{aligned} &\lim_{t\to\infty} \mathbb{P}\left(\frac{X_t}{t} \le x, \frac{Y_t}{t} \le y\right) \\ &= \int_{-\infty}^{x} du \int_{-\infty}^{y} dv\, f_1(u,v) \left\{g_1(u,v) + g_2(u,v)\right\} \eta_1(u,v;\alpha,\beta,\gamma,\delta) I_{\mathcal{D}_1}(u,v), \end{aligned} \tag{21}$$

where x, y are real numbers and

$$f_1(x,y) = \frac{1}{\pi^2(1-4x^2)(1-4y^2)\sqrt{D_1(x,y)}}, \tag{22}$$

$$D_1(x,y) = 81(x^4+y^4) - 18x^2y^2 - 18(x^2+y^2) + 1, \tag{23}$$

$$g_1(x,y) = \Big\{648(x^4+y^4) + 576x^2y^2 - 324(x^2+y^2) + 53 + 4\left\{7 - 18(x^2+y^2)\right\}\sqrt{D_1(x,y)}\Big\}^{\frac{1}{2}}, \tag{24}$$

$$g_2(x,y) = \Big\{648(x^4+y^4) + 576x^2y^2 - 324(x^2+y^2) + 53 - 4\left\{7 - 18(x^2+y^2)\right\}\sqrt{D_1(x,y)}\Big\}^{\frac{1}{2}}, \tag{25}$$

$$\eta_1(x,y;\alpha,\beta,\gamma,\delta) = 1 - 2x\Big[|\alpha|^2 - |\delta|^2 + \Re\left\{(-\alpha+\gamma-\delta)\overline{\beta} + (\alpha+\beta-\delta)\overline{\gamma}\right\}\Big] + 2y\Big[|\beta|^2 - |\gamma|^2 + \Re\left\{(\beta+\gamma+\delta)\overline{\alpha} + (\alpha-\beta+\gamma)\overline{\delta}\right\}\Big], \tag{26}$$

$$I_{\mathcal{D}_1}(x,y) = \begin{cases} 1 & \left(D_1(|x|,|y|) > 0,\ 0 \le |x|,|y| \le \frac{1}{3}\right), \\ 0 & (otherwise). \end{cases} \tag{27}$$

One can note that the function $D_1(x,y)$ takes a biquadratic form and determines the shape of the compact support. To check the result numerically, we show in Figs. 2(a) and (b) the result obtained after a finite time of walking and the limit density function, respectively. Very similar features are visible and in particular the expected delocalisation is clearly confirmed. Since the distribution shown in Fig. 2(a) captures the state of the walker at time $t = 100$, not all features of the long time limit are developed as clearly as in the limit density function, however the overall form and asymmetry already coincide.

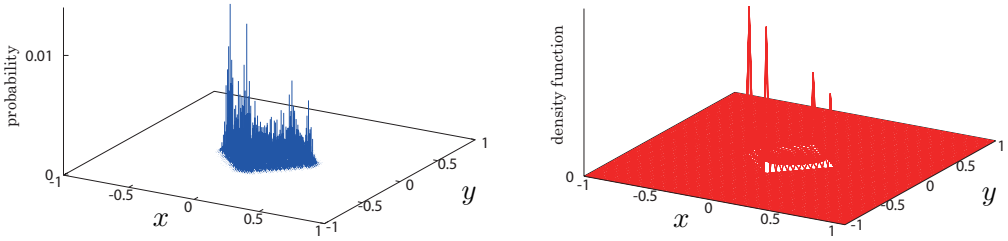

(a) $\mathbb{P}\left[\left(\frac{X_t}{t}, \frac{Y_t}{t}\right) = (x,y)\right]$ (b) limit density function

Fig. 2. Quantum walk using the coin operator given in Eq. (20). Figure (a) shows the probability distribution $\mathbb{P}\left[\left(\frac{X_t}{t}, \frac{Y_t}{t}\right) = (x,y)\right]$ at time $t = 100$ and Figure (b) shows the limit density function as $t \to \infty$. Here $\alpha = -\delta = \frac{1}{2}$, $\beta = \gamma = \frac{i}{2}$.

Proof. We can derive the above limit theorem using Fourier analysis [16]. For this, one starts off with the Fourier transform of the walker at time t,

$$|\hat{\Psi}_t(k_x,k_y)\rangle = \sum_{(x,y)\in\mathbb{Z}^2} e^{-i(k_x x+k_y y)}\,|\psi_t(x,y)\rangle\,, \tag{28}$$

with $k_x, k_y \in [-\pi,\pi)$. Equation (2) then determines the time evolution of the Fourier transform as

$$|\hat{\Psi}_{t+1}(k_x,k_y)\rangle = \hat{U}(k_x,k_y)\,|\hat{\Psi}_t(k_x,k_y)\rangle\,, \tag{29}$$

where $\hat{U}(k_x,k_y) = \hat{R}(k_x,k_y)U$ and

$$\hat{R}(k_x,k_y) = \begin{bmatrix} e^{ik_x} & 0 & 0 & 0 \\ 0 & e^{-ik_y} & 0 & 0 \\ 0 & 0 & e^{ik_y} & 0 \\ 0 & 0 & 0 & e^{-ik_x} \end{bmatrix}. \tag{30}$$

From the recurrence relation given by Eq. (29), one can obtain

$$|\hat{\Psi}_t(k_x,k_y)\rangle = \hat{U}(k_x,k_y)^t\,|\hat{\Psi}_0(k_x,k_y)\rangle\,, \tag{31}$$

and the eigenvalues $\lambda_j(k_x,k_y)$ and the normalized eigenvectors $|v_j(k_x,k_y)\rangle$ $(j=1,2,3,4)$ of the matrix $\hat{U}(k_x,k_y)$ can be used to express the (r_1,r_2)-th joint moments $(r_1,r_2=0,1,2,\ldots)$ of the random variable (X_t,Y_t) as

$$\begin{aligned}
\mathbb{E}(X_t^{r_1}Y_t^{r_2}) &= \sum_{(x,y)\in\mathbb{Z}^2} x^{r_1}y^{r_2}\mathbb{P}[(X_t,Y_t)=(x,y)] \\
&= \int_{-\pi}^{\pi}\frac{dk_x}{2\pi}\int_{-\pi}^{\pi}\frac{dk_y}{2\pi}\,\langle\hat{\Psi}_t(k_x,k_y)|D_x^{r_1}D_y^{r_2}|\hat{\Psi}_t(k_x,k_y)\rangle \\
&= (t)_{r_1+r_2}\int_{-\pi}^{\pi}\frac{dk_x}{2\pi}\int_{-\pi}^{\pi}\frac{dk_y}{2\pi}\sum_{j=1}^{4}\left\{\frac{D_x\lambda_j(k_x,k_y)}{\lambda_j(k_x,k_y)}\right\}^{r_1} \\
&\quad\times\left\{\frac{D_y\lambda_j(k_x,k_y)}{\lambda_j(k_x,k_y)}\right\}^{r_2}\left|\langle v_j(k_x,k_y)|\hat{\Psi}_0(k_x,k_y)\rangle\right|^2 \\
&\quad + O(t^{r_1+r_2-1})
\end{aligned} \tag{32}$$

with $D_x = i(\partial/\partial k_x)$, $D_y = i(\partial/\partial k_y)$ and $(t)_r = t(t-1)\times\cdots\times(t-r+1)$. Here, $\mathbb{E}(X)$ denotes the expected value of the random variable X. Introducing a function

$$\theta_1(k_x,k_y) = \frac{1}{2}\arcsin\left(\frac{2}{3}\sin k_x\cos k_y\right), \tag{33}$$

we have the eigenvalues

$$\lambda_1(k_x,k_y) = e^{i\theta_1(k_x,k_y)}, \quad \lambda_2(k_x,k_y) = -e^{i\theta_1(k_x,k_y)}, \tag{34}$$

$$\lambda_3(k_x,k_y) = ie^{-i\theta_1(k_x,k_y)}, \quad \lambda_4(k_x,k_y) = -ie^{-i\theta_1(k_x,k_y)}. \tag{35}$$

Hence, the functions $D_x\lambda_j(k_x,k_y)/\lambda_j(k_x,k_y)$ and $D_y\lambda_j(k_x,k_y)/\lambda_j(k_x,k_y)$ are computed as follows.

$$\frac{D_x\lambda_j(k_x,k_y)}{\lambda_j(k_x,k_y)} = \begin{cases} -\frac{\cos k_x \cos k_y}{\sqrt{9-4\sin^2 k_x \cos^2 k_y}} & (j=1,2), \\ \frac{\cos k_x \cos k_y}{\sqrt{9-4\sin^2 k_x \cos^2 k_y}} & (j=3,4), \end{cases} \tag{36}$$

$$\frac{D_y\lambda_j(k_x,k_y)}{\lambda_j(k_x,k_y)} = \begin{cases} \frac{\sin k_x \sin k_y}{\sqrt{9-4\sin^2 k_x \cos^2 k_y}} & (j=1,2), \\ -\frac{\sin k_x \sin k_y}{\sqrt{9-4\sin^2 k_x \cos^2 k_y}} & (j=3,4). \end{cases} \tag{37}$$

The eigenvector associated to the eigenvalue $\lambda_j(k_x,k_y)$ has an expression

$$\begin{bmatrix} -e^{ik_x}\left\{\sqrt{3}e^{ik_y}\lambda_j(k_x,k_y)^2 + (e^{2ik_y}-1)\lambda_j(k_x,k_y) + \sqrt{3}e^{ik_y}\right\} \\ \sqrt{3}\lambda_j(k_x,k_y)^2 - (e^{ik_x}+e^{ik_y})\lambda_j(k_x,k_y) - \sqrt{3}e^{i(k_x+k_y)} \\ -e^{ik_y}\left[\sqrt{3}e^{ik_y}\lambda_j(k_x,k_y)^2 + \left\{e^{i(k_x+k_y)}+1\right\}\lambda_j(k_x,k_y) - \sqrt{3}e^{ik_x}\right] \\ \lambda_j(k_x,k_y)\left\{3e^{ik_y}\lambda_j(k_x,k_y)^2 - e^{ik_x} - e^{i(k_x+2k_y)} + e^{ik_y}\right\} \end{bmatrix}, \tag{38}$$

from which we get the normalized eigenvector $|v_j(k_x,k_y)\rangle$ to compute the moments. Using the information above, one can see from Eq. (32) that $\mathbb{E}(X_t^{r_1}Y_t^{r_2})/t^{r_1+r_2}$ converges as $t\to\infty$, which allows to determine the rescaled position of the walker $(X_t/t, Y_t/t)$. By setting $D_x\lambda_j(k_x,k_y)/\lambda_j(k_x,k_y) = x, D_y\lambda_j(k_x,k_y)/\lambda_j(k_x,k_y) = y$ after $t\to\infty$ in the joint moments $\mathbb{E}[(X_t/t)^{r_1}(Y_t/t)^{r_2}]$, one gets a convergence theorem

$$\begin{aligned} &\lim_{t\to\infty}\mathbb{E}\left[\left(\frac{X_t}{t}\right)^{r_1}\left(\frac{Y_t}{t}\right)^{r_2}\right] \\ &= \int_{-\pi}^{\pi}\frac{dk_x}{2\pi}\int_{-\pi}^{\pi}\frac{dk_y}{2\pi}\sum_{j=1}^{4}\left\{\frac{D_x\lambda_j(k_x,k_y)}{\lambda_j(k_x,k_y)}\right\}^{r_1}\left\{\frac{D_y\lambda_j(k_x,k_y)}{\lambda_j(k_x,k_y)}\right\}^{r_2}\left|\langle v_j(k_x,k_y)|\hat{\Psi}_0(k_x,k_y)\rangle\right|^2 \\ &= \int_{-\infty}^{\infty}dx\int_{-\infty}^{\infty}dy\; x^{r_1}y^{r_2}f_1(x,y)\left\{g_1(x,y)+g_2(x,y)\right\}\eta_1(x,y;\alpha,\beta,\gamma,\delta)I_{\mathcal{D}_1}(x,y), \end{aligned} \tag{39}$$

which guarantees Theorem 1 (See also Eq. (13) in the paper [14]). □.

3.2 Quadratic compact support type

Another interesting two-dimensional quantum walk for which a limit theorem can be derived is the walk using the coin-flip operation

$$U = \frac{1}{\sqrt{2}}\begin{bmatrix} 0 & -1 & 1 & 0 \\ 1 & 0 & 0 & -1 \\ 1 & 0 & 0 & 1 \\ 0 & 1 & 1 & 0 \end{bmatrix}. \tag{40}$$

Theorem 2 *For the quantum walk governed by the coin-flip operator in Eq.* (40)*, one can find the following long-time limit distribution.*

$$\lim_{t\to\infty}\mathbb{P}\left(\frac{X_t}{t}\le x,\ \frac{Y_t}{t}\le y\right) = \int_{-\infty}^{x}du\int_{-\infty}^{y}dv\, f_2(u,v)\eta_2(u,v;\alpha,\beta,\gamma,\delta)I_{\mathcal{D}_2}(u,v), \tag{41}$$

where x, y are real numbers and

$$f_2(x,y) = \frac{4}{\pi^2(1-4x^2)(1-4y^2)}, \tag{42}$$

$$\eta_2(x,y;\alpha,\beta,\gamma,\delta) = 1 - 2x\left\{|\alpha|^2 - |\delta|^2 - 2\Re(\beta\bar{\gamma})\right\} + 2y\left\{|\beta|^2 - |\gamma|^2 - 2\Re(\alpha\bar{\delta})\right\}, \tag{43}$$

$$I_{\mathcal{D}_2}(x,y) = \begin{cases} 1 & \left(x^2+y^2 < \frac{1}{4}\right), \\ 0 & (otherwise). \end{cases} \tag{44}$$

Note that the compact support of the limit density function is given by a quadratic equation whereas for the coin discussed in Theorem 1 it was of the form of a biquadratic equation. Comparing the compact supports obtained for the walks using Eq. (40) and using the Grover coin [14], one can note that they are identical. However, the limit density function is fundamentally different due to the absence of a Dirac δ-function.

We show a finite time probability distribution and the limit density function in Fig. 3 and one can again see that the limit density function reproduces the characteristic features of the probability distribution from the discrete-time evolution.

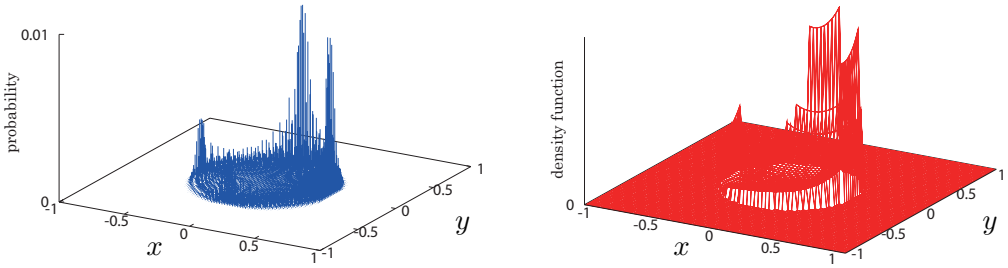

(a) $\mathbb{P}\left[\left(\frac{X_t}{t}, \frac{Y_t}{t}\right) = (x,y)\right]$ (b) limit density function

Fig. 3. Quantum walk using the coin operator given in Eq. (40). Figure (a) shows the probability distribution $\mathbb{P}\left[\left(\frac{X_t}{t}, \frac{Y_t}{t}\right) = (x,y)\right]$ at time $t = 100$ and Figure (b) shows the limit density function as $t \to \infty$. Here $\alpha = -\delta = \frac{1}{2}$, $\beta = \gamma = \frac{i}{2}$.

Proof. This theorem can be proven in a manner very similar to the one used for Theorem 1. The information that we need to compute the limit of the moments $\mathbb{E}[(X_t/t)^{r_1}(Y_t/t)^{r_2}]$ as $t \to \infty$, is shown as follows. The unitary matrix $\hat{U}(k_x,k_y) = \hat{R}(k_x,k_y)U$ has four different eigenvalues

$$\lambda_1(k_x,k_y) = e^{i\theta_2(k_x,k_y)}, \quad \lambda_2(k_x,k_y) = -e^{i\theta_2(k_x,k_y)}, \tag{45}$$

$$\lambda_3(k_x,k_y) = ie^{-i\theta_2(k_x,k_y)}, \quad \lambda_4(k_x,k_y) = -ie^{-i\theta_2(k_x,k_y)}, \tag{46}$$

in which the function $\theta_2(k_x,k_y)$ is defined by

$$\theta_2(k_x,k_y) = \frac{1}{2}\arcsin(\cos k_x \sin k_y). \tag{47}$$

These eigenvalues give the functions in Eq. (32),

$$\frac{D_x\lambda_j(k_x,k_y)}{\lambda_j(k_x,k_y)} = \begin{cases} \frac{\sin k_x \sin k_y}{2\sqrt{1-\cos^2 k_x \sin^2 k_y}} & (j=1,2), \\ -\frac{\sin k_x \sin k_y}{2\sqrt{1-\cos^2 k_x \sin^2 k_y}} & (j=3,4), \end{cases} \tag{48}$$

$$\frac{D_y\lambda_j(k_x,k_y)}{\lambda_j(k_x,k_y)} = \begin{cases} -\frac{\cos k_x \cos k_y}{2\sqrt{1-\cos^2 k_x \sin^2 k_y}} & (j=1,2), \\ \frac{\cos k_x \cos k_y}{2\sqrt{1-\cos^2 k_x \sin^2 k_y}} & (j=3,4). \end{cases} \tag{49}$$

We, moreover, have an expression of the eigenvector

$$\begin{bmatrix} \lambda_j(k_x,k_y)e^{ik_x}(e^{2ik_y}+1) \\ -\sqrt{2}\left\{\lambda_j(k_x,k_y)^2 - e^{i(k_x+k_y)}\right\} \\ \sqrt{2}e^{ik_y}(e^{ik_y}\lambda_j(k_x,k_y)^2 + e^{ik_x}) \\ \lambda_j(k_x,k_y)\left\{2e^{ik_y}\lambda_j(k_x,k_y)^2 - e^{i(k_x+2k_y)} + e^{ik_x}\right\} \end{bmatrix}, \tag{50}$$

which associates to the eigenvalue $\lambda_j(k_x,k_y)$ $(j \in \{1,2,3,4\})$. □.

4 Summary

In this work we have examined two different kinds of quantum walks on a two-dimensional lattice. One of the coin-flip operators used for the walk was previously introduced as a nonrepeating coin-flip operation [15] whereas, the other one used here can be viewed as a specific subset of the nonrepeating coin operation. However, the long-time limit distribution is obtained for the first time for the quantum walk using either Eq. (20) or Eq. (40). These walks constitute a new class of quantum walks with unique properties compared to the two-dimensional walks whose coin-flip operator is given by a parameterized coin operation that contains a Grover coin. We have presented numerical results for finite-time evolution and long-time limit density functions for these walks in rescaled coordinates $(X_t/t, Y_t/t)$. Apart from giving the explicit forms of the walks and the associated limit theorems, one of our main findings is that both these forms of quantum walks result in delocalisation of the distribution for initial states that show localisation for evolutions using the Grover coin operation. This can be clearly seen from the numerically obtained probability distributions and has been analytically confirmed by the absence of the term containing a Dirac δ-function in the limit distributions. Again, our limit theorems prove that the quantum walks have ballistically spreading distributions which result in delocalisation, with the exact form given in a closed mathematical form. Each of the exact forms has a unique compact support and exactly expresses the shape of the region where the walker can be observed after the long-time dynamics. While the shape of the compact support for the quantum walk whose coin-flip operator given by Eq. (20) looks like a square from the numerical analysis, it is in fact a biquadratic shape. The limit distribution therefore delivers an insight that the numerical experiment cannot give.

While we have shown the existence of two limit distributions different from the one of the Grover walk, we speculate that there are many undescribed types of walks which possess unique distributions and it is a challenging task to describe them from a mathematical view

point. From the theorems shown in this paper, we can expect that it would be hard to compute a limit theorem for the quantum walk defined by more general coin operations, but, we hope that the long-time limit distributions presented here will stimulate future works.

Acknowledgements

TM acknowledges support from the Japan Society for the Promotion of Science. NK acknowledges financial support of the Grant-in-Aid for Scientific Research (C) of Japan Society for the Promotion of Science (Grant No. 21540118). This work was supported by the Okinawa Institute of Science and Technology Graduate University.

References

1. G. Riazanov (1958), *The feynman path integral for the dirac equation*, Soviet Journal of Experimental and Theoretical Physics, 6, 1107.
2. R.P. Feynman (1986), *Quantum mechanical computers*, Foundations of physics, 16(6), pp. 507–531.
3. K.R. Parthasarathy (1988), *The passage from random walk to diffusion in quantum probability*, Journal of applied probability, pp. 151–166.
4. Y. Aharonov, L. Davidovich and N. Zagury (1993), *Quantum random walks*, Phys. Rev. A, 48(2), pp. 1687–1690.
5. D.A. Meyer (1996), *From quantum cellular automata to quantum lattice gases*, Journal of Statistical Physics, 85(5-6), pp. 551–574.
6. A. Ambainis, E. Bach, A. Nayak, A. Vishwanath and J. Watrous One-dimensional quantum walks. In: Proceedings of the thirty-third annual ACM symposium on Theory of computing, ACM, (2001), pp. 37–49.
7. A. Nayak and A. Vishwanath Quantum walk on the line. Technical Report 43, DIMACS, (2000).
8. N. Konno (2002), *Quantum random walks in one dimension*, Quantum Information Processing, 1(5), pp. 345–354.
9. S.E. Venegas-Andraca (2012), *Quantum walks: a comprehensive review*, Quantum Information Processing, 11(5), pp. 1015–1106.
10. A. Peruzzo, M. Lobino, J. C. F. Matthews, N. Matsuda, A. Politi, K. Poulios, X. Zhou, Y. Lahini, N. Ismail, K. Wörhoff, Y. Bromberg, Y. Silberberg, M. G. Thompson, J. L. OBrien 2010, *Quantum Walks of Correlated Photons* Science **329** (5998): 1500–1503.
11. J. O. Owens, M. A. Broome, D. N. Biggerstaff, M. E. Goggin, A. Fedrizzi, T. Linjordet, M. Ams, G. D. Marshall, J. Twamley, M. J. Withford, and A. G. White 2011, *Two-photon quantum walks in an elliptical direct-write waveguide array*, New J. Phys. **13** 075003
12. A. Schreiber, A. Gábris, P. P. Rohde, K. Laiho, M. Štefanák, V. Potocek, C. Hamilton, I. Jex, C. Silberhorn 2012, *A 2D Quantum Walk Simulation of Two-Particle Dynamics* Science **336** (6077): 55–58.
13. L. Sansoni, F. Sciarrino, G. Vallone, P. Mataloni, A. Crespi, R. Ramponi, and R. Osellame (2012), *Two-Particle Bosonic-Fermionic Quantum Walk via Integrated Photonics*, Phys. Rev. Lett. **108**, 010502.
14. K. Watabe, N. Kobayashi, M. Katori and N. Konno (2008), *Limit distributions of two-dimensional quantum walks*, Phys. Rev. A, 77(6), 062331.
15. T.J. Proctor, K.E. Barr, B. Hanson, S. Martiel, PavloviV. ć, A. Bullivant and V.M. Kendon (2014), *Nonreversal and nonrepeating quantum walks*, Phys. Rev. A, 89, 042332.
16. G. Grimmett, S. Janson and P.F. Scudo (2004), *Weak limits for quantum random walks*, Phys. Rev. E, 69(2), 026119.